# Coordinated Traffic Flow Control in a Connected Environment

December 2023

A Research Report from the National Center for Sustainable Transportation

Tianchen Yuan, University of Southern California

Petros A. Ioannou, University of Southern California

National Center for Sustainable Transportation
A USDOT University Transportation Center

METRANS Transportation Consortium
USC | CSULB

# TECHNICAL REPORT DOCUMENTATION PAGE

| | | |
|---|---|---|
| **1. Report No.**<br>NCST-USC-RR-23-34 | **2. Government Accession No.**<br>N/A | **3. Recipient's Catalog No.**<br>N/A |
| **4. Title and Subtitle**<br>Coordinated Traffic Flow Control in a Connected Environment | | **5. Report Date**<br>December 2023 |
| | | **6. Performing Organization Code**<br>N/A |
| **7. Author(s)**<br>Tianchen Yuan, Ph.D. Candidate, https://orcid.org/0000-0003-4599-2587<br>Petros Ioannou, Ph.D., https://orcid.org/0000-0001-6981-0704 | | **8. Performing Organization Report No.**<br>N/A |
| **9. Performing Organization Name and Address**<br>University of Southern California<br>METRANS Transportation Consortium<br>University Park Campus, VKC 367 MC:0626<br>Los Angeles, California 90089-0626. | | **10. Work Unit No.**<br>N/A |
| | | **11. Contract or Grant No.**<br>USDOT Grant 69A3551747114 |
| **12. Sponsoring Agency Name and Address**<br>U.S. Department of Transportation<br>Office of the Assistant Secretary for Research and Technology<br>1200 New Jersey Avenue, SE, Washington, DC 20590 | | **13. Type of Report and Period Covered**<br>Final Research Report (August 2021 – June 2023) |
| | | **14. Sponsoring Agency Code**<br>USDOT OST-R |

**15. Supplementary Notes**
DOI: https://doi.org/10.7922/G2B27SNS
Dataset DOI: https://doi.org/10.7910/DVN/4GK5MW


**16. Abstract**
Freeway and arterial transportation networks in most districts are managed separately without any coordination. This lack of coordination increases the severity of traffic congestion when one or both systems reach their capacities. Some field studies have observed reductions in travel time by coordinating freeway ramps with adjacent arterial signals. To advance the investigation, we propose an integrated traffic management strategy that involves variable speed limit, lane change, ramp metering for freeway traffic flow control, and a traffic-responsive signal control scheme for adjacent traffic light intersections. The variable speed limit and lane change control are designed to alleviate congestion at a lane-drop bottleneck in an arbitrary section, and reject potential uncertainties from measurements or model parameters. The ramp metering algorithm takes advantage of the signal plan of neighboring arterial intersection when estimating on-ramp demands. The signal plan for each arterial intersection is determined by a simulation-based cycle length model and estimated demands of all directions, part of which depend on off-ramp flow measurements. The above data sharing mechanism strengthens the connection between the freeway and arterial networks and enhances the control performance. We demonstrate the effectiveness and quantify the benefits provided by the proposed system in terms of traffic mobility, safety and emission using microscopic traffic simulations.


| | | | |
|---|---|---|---|
| **17. Key Words**<br>Variable speed limit, lane change, ramp metering, traffic signal control, coordination | | **18. Distribution Statement**<br>No restrictions. | |
| **19. Security Classif. (of this report)**<br>Unclassified | **20. Security Classif. (of this page)**<br>Unclassified | **21. No. of Pages**<br>36 | **22. Price**<br>N/A |

Form DOT F 1700.7 (8-72) Reproduction of completed page authorized

NCST

## About the National Center for Sustainable Transportation

The National Center for Sustainable Transportation is a consortium of leading universities committed to advancing an environmentally sustainable transportation system through cutting-edge research, direct policy engagement, and education of our future leaders. Consortium members include: the University of California, Davis; California State University, Long Beach; Georgia Institute of Technology; Texas Southern University; the University of California, Riverside; the University of Southern California; and the University of Vermont. More information can be found at: ncst.ucdavis.edu.

## Disclaimer

The contents of this report reflect the views of the authors, who are responsible for the facts and the accuracy of the information presented herein. This document is disseminated in the interest of information exchange. The report is funded, partially or entirely, by a grant from the U.S. Department of Transportation's University Transportation Centers Program. However, the U.S. Government assumes no liability for the contents or use thereof.

The U.S. Department of Transportation requires that all University Transportation Center reports be published publicly. To fulfill this requirement, the National Center for Sustainable Transportation publishes reports on the University of California open access publication repository, eScholarship. The authors may copyright any books, publications, or other copyrightable materials developed in the course of, or under, or as a result of the funding grant; however, the U.S. Department of Transportation reserves a royalty-free, nonexclusive and irrevocable license to reproduce, publish, or otherwise use and to authorize others to use the work for government purposes.

## Acknowledgments

This study was funded, partially or entirely, by a grant from the National Center for Sustainable Transportation (NCST), supported by the U.S. Department of Transportation (USDOT) through the University Transportation Centers program. The authors would like to thank the NCST and the USDOT for their support of university-based research in transportation, and especially for the funding provided in support of this project.

NCST

# Coordinated Traffic Flow Control in a Connected Environment

A National Center for Sustainable Transportation Research Report

December 2023

**Tianchen Yuan,** Department of Electrical Engineering, University of Southern California

**Petros A. Ioannou,** Department of Electrical Engineering, University of Southern California

NCST

[page intentionally left blank]

# TABLE OF CONTENTS

# List of Tables

## List of Figures

# Coordinated Traffic Flow Control in a Connected Environment

## EXECUTIVE SUMMARY

The current traffic system operates most of the time as an open loop dynamical system with control actions limited to traffic light control at intersections of arterial streets and ramps to highways. These control actions rely on limited sensor data to make decisions which are often far for the optimum. In the case of ramps, the control metering switches off when the ramp queue exceeds certain capacity which takes place usually during peak times when control is needed the most. As the traffic demand increases the current situation is not sustainable as congestion will get worse and inefficiencies increase unless new sensor technologies and traffic flow control techniques are developed.

The deployment of vehicle to infrastructure (V2I) and vehicle to vehicle (V2V) technologies is the inevitable choice that will open the way to a revolution in traffic flow control and optimization as connectivity will enable the design of accurate traffic control techniques to better control traffic and prevent the onset of congestion.

The purpose of this project is to investigate how connectivity provided by such communication technologies can be used to develop traffic flow control systems that will enhance mobility, safety, and provide positive benefits to transportation efficiency and environment. We propose a coordinated traffic flow control system that consists of four components: variable speed limit (VSL), lane change (LC) and ramp metering (RM) control as well as traffic signal control (TSC) of adjacent intersections affecting or affected by ramp traffic from the highway. We use cell transmission model (CTM) to capture freeway traffic dynamics due to its simplicity and reasonable accuracy. The freeway segment of interest is divided into multiple homogeneous sections under the CTM framework. The VSL controller computes the speed limit recommendations for each CTM section using measured flows and densities in a feedback manner and communicates them to the upstream vehicles. It is designed to dissipate freeway bottleneck congestion at an arbitrary location with the proper choice of deployment location and the assistance from LC and RM control. As for the arterials, we design a traffic-responsive traffic signal controller (TSC) that computes the cycle length based on a modified Webster model, and then computes the split using estimated traffic flow ratio.

Each control component requires some information from others as part of the control input except LC. The VSL control requires the on-ramp and off-ramp flow rate when computing the desired inflow for each CTM section. The RM algorithm estimates the on-ramp demand using arterial signal plans and traffic flow data. The TSC requires the off-ramp flow rate to estimate the flow ratio of each phase. The above data-sharing and coordination mechanism improves the accuracy of traffic states estimation and the efficiency of the overall traffic control.

The proposed integrated controller is simulated using a microscopic traffic simulator based on the commercial software PTV Vissim 10. The simulation road network contains a 16-km

segment of I-710 freeway and the adjacent arterial region in Los Angeles, California, United States. The freeway segment has 5 lanes, 5 on-ramps and 5 off-ramps. All ramps are connected with the arterial road network. There are 7 arterial intersections aligned in parallel with the freeway. Vehicle inputs are generated from one freeway entrance and 16 arterial entrances based on the traffic data of April 2019 from PeMS. The traffic simulation model is integrated with the emission model MOVES provided by the Environment Protection Agency (EPA) to calculate the average emission rates of vehicles in each microscopic simulation. The integrated controller is evaluated in a free flow scenario as well as two incident scenarios in terms of the average travel time (ATT), the average number of stops and the emission rates of $CO_2$. Ten independent Monte-Carlo simulations for each combination of scenario and control method are carried out and results are averaged in order to reduce randomness and improve reliability.

As expected, the coordination mechanism does not produce significant benefits under free flow conditions. However, when the road network is under the pressure of incidents and congestion, the coordinated control reduces the travel time and the emission for the affected region compared with individual control. For example, when a freeway lane closure affects both the freeway travel and the on-ramp merging, the coordinated control improves the freeway travel time by 7% and the arterial travel time by 10%.

## Introduction

Demand for freeway and arterial travel grows in a fast pace as the population increases in metropolitan areas worldwide, leading to traffic congestion and delays at sensitive parts of road networks such as ramps and intersections. Research efforts on freeway [1-3] and arterial traffic management [4-6] as separate entities have both achieved certain levels of success in terms of reducing travel time, collision risks and emissions. However, the joint control of freeway and arterial traffic has been rarely explored due to the difficulty of modeling two completely different traffic patterns and high complexity of the road network. In practice, the coordinated operation of freeways and adjacent arterials is hindered by the fact that the two facilities are typically managed by two separate authorities with different objectives and limited communications [7]. Despite the above-mentioned restrictions, some field-based studies have verified the effectiveness of coordinating freeway ramp metering (RM) with adjacent arterial traffic signals [8-10], which can be considered as a preliminary step of coordinating freeway and arterial (CFA) operations and reveals the great potential of CFA on improving traffic operation efficiency.

Popular freeway traffic control techniques include variable speed limit (VSL) control, lane change (LC) control and ramp metering (RM). During the last few decades research efforts focused on one or a combination of the above three methods to alleviate congestion at freeway bottlenecks. The VSL controller regulates the traffic flow via variable speed commands in order to protect the bottleneck flow to stay at its maximum possible value and reduce the effect of capacity drop [11]. VSL control techniques designed using macroscopic models failed to take into account the forced lane changes at the bottleneck leading to capacity drop which VSL control cannot effectively handle [12-14]. To address this issue, LC recommendations are used at the upstream area of the bottleneck to guide the vehicles onto open lanes in advance and reduce the forced lane changes and the consequential capacity drop [15]. Ramp metering controls the inflow of traffic to the freeway lanes by adjusting the traffic signal timing at each on-ramp entrance. Despite the promising effect of RM in theory [1, 16], the on-ramp space is frequently saturated during peak hours, which forces RM to switch off offering no benefits when it is needed the most. Although alternative solutions which consider the balance of freeway occupancy and on-ramp queue length have been proposed [17, 18], the improvement is still limited when both freeway traffic and on-ramp demands are high.

The above facts motivate us to examine a more intuitive solution by connecting the ramps with adjacent arterial road networks and using arterial traffic signals to assist the management of on-ramp demands, as pointed out by a few CFA studies [9, 19]. We extend these efforts by integrating all the previous mentioned freeway traffic regulation techniques (VSL, LC, RM) with arterial traffic signal control (TSC) to mitigate congestion for a complex road network involving freeway and adjacent arterial intersections under different demand levels and incident scenarios.

## Literature Review

Among numerous freeway traffic management schemes, variable speed limit (VSL) control and ramp metering (RM) have been widely studied due to their easy implementation and significant benefits in traffic mobility, safety, and environment impact.

Early VSL control designs aimed at stabilizing mainstream traffic flows and minimizing speed variations with reactive rule-based logic [20, 21]. The reactive nature of these approaches introduces time lags between VSL actions and traffic conditions, and thus, leads to limited performance in terms of travel time and energy consumption. In contrast, many recent developed VSL algorithms compute the speed commands by solving an optimization problem at each time step based on predictions of future traffic states using model predictive control (MPC) techniques [22-25]. The objective function to be optimized typically consists of total travel time, safety measurements, emission rates and fuel consumption. Although MPC-based approaches improve the control performance by eliminating time lags of VSL command activation compared to reactive rule-based approaches, they do not guarantee the stability of vehicle densities and require substantial computational efforts when applied to large-scale road networks. Another well-known alternative is to design a feedback law to compute appropriate speed limits using current and past traffic states [26-28], which consumes much less computational efforts than MPC-based approaches. In addition, feedback-based VSL controller guarantees the convergence of mainstream traffic flows and densities analytically [29]. However, feedback-based approaches rely on accurate measurements of traffic states to generate effective control actions. A small deviation from the true value on sensitive variables, vehicle densities for example, may produce unsatisfactory closed-loop behaviors [30]. To address the issue, Alasiri et al. proposed a robust VSL algorithm to treat the uncertainties as a variable in the traffic model and eliminate it with proportional-integral (PI) control [31]. The design was based on a single cell transmission model (CTM) section without ramps.

The deployment location of VSL signs is a crucial design parameter but has been neglected by most of the above studies. Latest research developed some standards on placing VSL signs in order to achieve optimal control performance [11, 32-34]. In [32], the authors claimed that VSL signs should be placed at locations so there is enough space for vehicles to accelerate and reach the bottleneck capacity. In [33], VSL signs were placed at locations in an effort to minimize collision risks at freeway recurrent bottlenecks. In [34], Martinez and Jin defined the "optimal" location as the minimum discharging distance to prevent capacity drop, based on which they formulated an optimization problem using a variation of Lighthill-Whitham-Richards (LWR) model. However, the minimum discharging distance may not necessarily produce the best performance in terms of travel time, safety and emission. In [11], a lower bound of the upstream VSL zone distance was developed using rigorous analysis and simulation verification based on an idealized freeway network without considering ramps.

Since ramps connect freeways with arterial streets, a well-designed ramp metering strategy should be able to improve the traffic mobility of both regions. Some isolated RM algorithms were first proposed in 1990s [35, 36], including the famous ALINEA [16], which takes freeway occupancy as input and computes the metering rate in a local feedback control manner. The

classic ALINEA does not consider the potential spillback of on-ramp queues under high traffic demands. Therefore, it was modified in [17] to avoid the overextension of on-ramp queues by including both the mainstream occupancy and the queue length in the feedback loop. Due to the fact that ramp flows are also affected by the mainstream traffic, coordinated RM algorithms that take into account both local and system-wide traffic conditions typically outperform isolated RM algorithms. In [37], Paesani et al. proposed a system-wide adaptive RM algorithm to compute the metering rates based on estimated future traffic states with linear regression. The lack of accurate real time data makes such methods deviate considerably from the theoretical best performance. In [38], another extension of ALINEA was made by connecting all the on-ramps via a central controller and dynamically distribute the ramp demands. When one on-ramp queue reaches the threshold, the central controller increases the throughput of this particular on-ramp while decreases the throughput of other on-ramps. In [39], a similar two-level structure was embedded into the RM algorithm. The upper-level controller determines the optimal total inflow using MPC framework, and the lower level controller distributes the computed total inflow to each on-ramp. Although improvement can be observed by coordinating each RM controller within the network, the control performance is still limited when heavy traffic exists in the mainstream, as RM only affects the vehicle density closely downstream of the on-ramp. This motivates the investigation of combining RM with mainstream traffic regulation techniques such as VSL and LC control.

To coordinate VSL and RM, Hegyi et al. proposed an optimization-based formulation with an objective function containing the total time spent (TTS) for the mainstream traffic and the on-ramp queue [40]. This framework has been adopted by many researchers since then to demonstrate the optimality of their proposed integrated controllers [1, 41-43]. As previously mentioned, optimization-based algorithms (mainly using MPC) are not applicable to large-scale road networks because the computation time increases rapidly with the network size [3]. To tackle this problem, several easy-to-implement integrated controllers have been proposed [3, 44, 45] based on shock wave theory, feedback control or logic rules. A common drawback of these algorithms is the lack of coordination between different types of controllers.

Traffic signal control (TSC) is considered as the most important and effective method to manage arterial traffic. Existing TSC strategies can be divided into two categories: fixed-time TSC and traffic-responsive TSC. Fixed-time TSC switches between predetermined signal programs according to the time of the day, and thus, suitable for stable, unsaturated traffic conditions. In [46, 47], F. V. Webster designed a signal timing model to minimize the travel delay and developed the basis for modern fixed-time TSC design. Two of the most widely implemented and extended fixed-time TSC strategies are MAXBAND [48] and TRANSYT [49]. MAXBAND coordinates traffic signals along an arterial with the same cycle length and proper offsets so that vehicles can travel without stopping, which formulates a progression band with a uniform bandwidth to be maximized. Representative extensions of MAXBAND include assigning multiple bandwidths for different road segments [50], incorporating route guidance [51], or speed advisory [4]. TRANSYT takes historical traffic data of the road network as input, and then determines the optimal signal control with a heuristic "hill climbing" algorithm. The major limitation of fixed-time TSC is that it cannot handle highly saturated traffic conditions or

incident scenarios, which prompts the study of real-time traffic-responsive TSC. In [52], a traffic-responsive version of TRANSYT - SCOOT, was developed to adjust signal cycles, splits and offsets with newly-measured traffic flows and occupancy. In [53], a real-time hierarchical optimized distributed effective system (RHODES) was proposed with two main operation processes. The first process uses sensor data to estimate future traffic flows within the network. The second process selects the optimal phasing time with dynamic programming (DP) and decision trees. Despite their satisfactory performance in numerous field tests, most traffic-responsive TSC systems rely on accurate real-time traffic data and a powerful central machine to solve optimization algorithms whose complexity grows exponentially with the size of the problem leading to costly implementation with restrictions on the size of arterial networks.

Due to limited on-ramp space it is difficult to maintain efficient freeway operations and avoid the spillback of ramp queues simultaneously with freeway traffic control only [7]. A promising solution is to coordinate freeway and arterial (CFA) traffic and utilize arterial road capacities to mitigate on-ramp or freeway congestion. However, very few research efforts have been made in this area due to the difficulty of modeling two completely different traffic patterns and high complexity of the road network. In [54, 55], separate models are developed to characterize the freeway part and the arterial regions, and then MPC-based control schemes are proposed to minimize the total time spent/delay. Both studies verified the performance improvement by having a centralized control over the mixed road network, but only RM and TSC are considered as traffic regulation techniques.

## Methodology

In this section, we propose an integrated control strategy to regulate the traffic in a road network consisting of both freeway and the adjacent arterial region (depicted in Figure 1) with the purpose of reducing the vehicle travel time, the emission rates, and the queue lengths of on-ramps and arterial intersections under all traffic conditions and input demand levels. Traffic data and control inputs are shared between the two systems to enhance the control performance. Note that all the freeway ramps are connected with arterial roads. Some connections are omitted in Figure 1 due to limited drawing space. More details of the road network configuration will be presented later in the section. The notations used hereafter are summarized in Table 1.

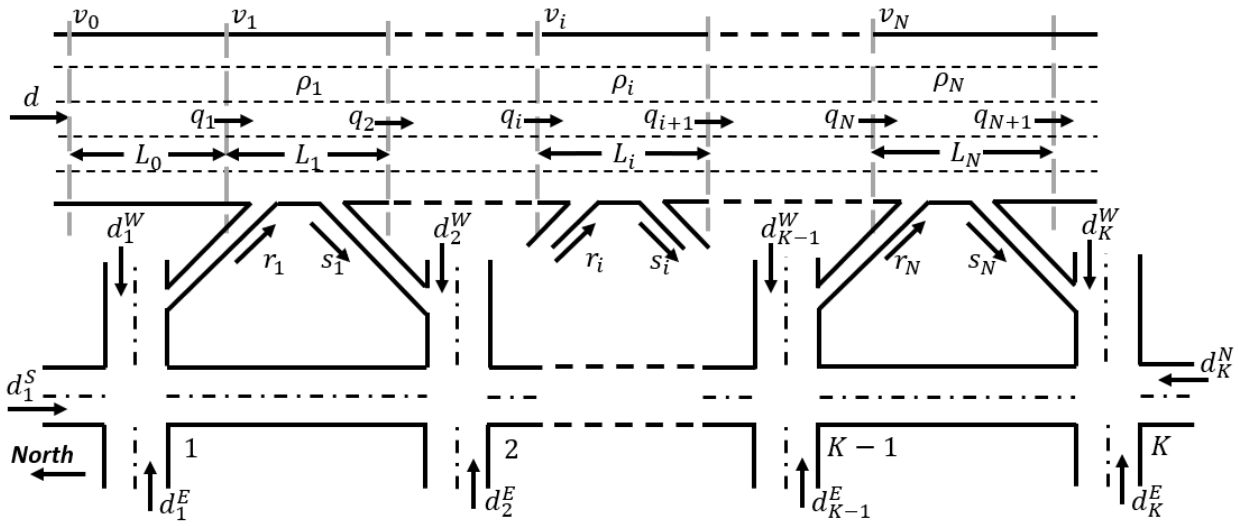


**Figure 1. Road network**

**Table 1. Definition of variables and model parameters**

| Symbol | Definition | Unit |
|---|---|---|
| $d$ | the freeway vehicle input | veh/h |
| $d_k^E$ | the vehicle input of arterial intersection $k$ with the direction specified by the superscript ($E$ stands for Eastbound) | veh/h |
| $C$ | the capacity of each section/cell | veh/h |
| $C_b$ | the bottleneck capacity | veh/h |
| $q_i$ | the mainstream inflow of freeway section $i$ | veh/h |
| $q_{i+1}$ | the mainstream outflow of freeway section $i$ | veh/h |
| $r_i$ | the on-ramp inflow of freeway section $i$ | veh/h |
| $s_i$ | the off-ramp outflow of freeway section $i$ | veh/h |
| $v_f$ | the free flow speed | km/h |
| $w$ | the back propagation speed | km/h |
| $\widetilde{w}$ | the rate that the outflow $q_{i+1}$ decreases with density $\rho_i$ when $\rho_i \geq \rho_c$ | km/h |
| $\rho_c$ | the critical density of the section/cell at which $v_f\rho_c = \widetilde{w}(\tilde{\rho}^j - \rho_c) = w(\rho^j - \rho_c) = C$ | veh/km |
| $\rho^j$ | the jam density at which the inflow $q_i$ decreases to 0 with rate $w$ | veh/km |
| $\tilde{\rho}^j$ | the jam density at which the outflow $q_{i+1}$ decreases to 0 with rate $\widetilde{w}$ | veh/km |
| $\rho_i$ | the density of freeway section $i$ | veh/km |
| $L_i$ | the length of freeway section $i$ | km |
| $\epsilon_0$ | the capacity drop factor, where $\epsilon_0 \in (0, 1)$ | unitless |

## Freeway Traffic Model

The Cell Transmission Model (CTM) is adopted to describe the traffic behaviors of the freeway segment because of its high computational efficiency and reasonable accuracy [29, 57-59] compared with higher-order models [60-62]. Under the framework of CTM, the selected freeway segment is divided into $N$ sections/cells and indexed from 1 to $N$ along the traffic flow direction, as shown in Figure 1. Each section/cell is characterized by the vehicle density, mainstream inflow, mainstream outflow, on-ramp inflow, off-ramp outflow and section length, denoted as $\rho_i, q_i, q_{i+1}, r_i, s_i, L_i$ respectively, where $i = 1, 2, \ldots, N$. Without loss of generality, it is assumed that an incident occurs and creates a bottleneck at section $M$ $(1 < M \leq N)$, as shown in Figure 2.

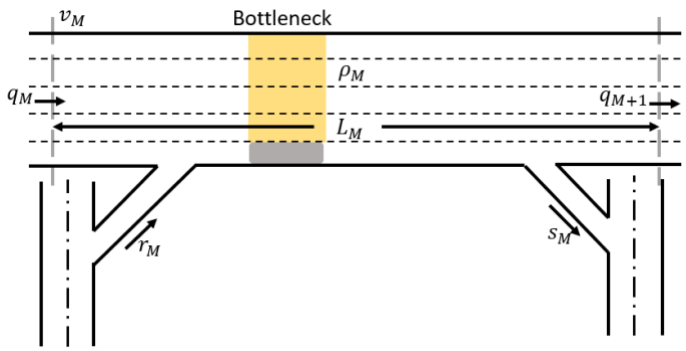


**Figure 2. Freeway bottleneck**

Although the original CTM can reproduce the traffic dynamics in normal circumstances, it does not capture the capacity drop phenomenon and bounded acceleration effects produced by forced lane change maneuvers at freeway bottlenecks or ramp merging areas [59, 63]. Nor does it consider the uncertainties in measured traffic states and model parameters. To address these issues and improve the consistency with microscopic observations, a modified multi-section CTM that accommodates the effect of both capacity drop and bounded acceleration is considered [29]. Moreover, the uncertainties in measurements and parameters are represented as an additional disturbance term $\mu_i$ in the conservation law of traffic flow [31]. Accordingly, the following equations describe the evolution of the vehicle density $\rho_i$ in each section:

$$\dot{\rho}_i = \frac{1}{L_i}(q_i - q_{i+1} + r_i - s_i + \mu_i) \qquad \text{for } i = 1, \dots, N \tag{1}$$

where

$$q_1 = \min\{d, C, w(\rho^j - \rho_1)\}$$
$$q_i = \min\{v_f \rho_{i-1}, \tilde{w}(\tilde{\rho}^j - \rho_{i-1}), C, w(\rho^j - \rho_i)\} \qquad \text{for } i = 2, \dots, M-1, M+2, \dots, N$$
$$q_M = \min\{v_f \rho_{M-1}, \tilde{w}(\tilde{\rho}^j - \rho_{M-1}), (1 - \epsilon(\rho_M))C_b, w(\rho^j - \rho_M)\}$$
$$q_{M+1} = \min\{v_f \rho_M, \tilde{w}(\tilde{\rho}^j - \rho_M), (1 - \epsilon(\rho_M))C_b, w(\rho^j - \rho_{M+1})\}$$
$$q_{N+1} = \min\{v_f \rho_N, \tilde{w}(\tilde{\rho}^j - \rho_N), C\}$$

and (2)

$$\epsilon(\rho_M) = \begin{cases} \epsilon_0 & \text{if } C_b < C \text{ and } \rho_M > \frac{C_b}{v_f} \\ 0 & \text{otherwise} \end{cases}$$

## Freeway Traffic Control

Based on the multi-section CTM presented above, this section aims to develop an integrated variable speed limit (VSL), lane change (LC) and ramp metering (RM) controller to guarantee all the mainstream sections operating under free-flow conditions, despite the existence of the bottleneck in arbitrary section $M$ $(1 < M \leq N)$. The VSL controller regulates the mainstream

inflow of each section so that the density converges to the desired value and the uncertainties are rejected. Lane change recommendations are provided for vehicles approaching the bottleneck in order to reduce the number of forced lane changes at very low speed in the vicinity of the bottleneck. The RM control is used to prevent mainstream traffic from being disturbed by large ramp input flows when the on-ramp capacity is not saturated.

### *Variable Speed Limit Control*

We propose a feedback-based VSL controller with the purpose of rejecting the disturbance $\mu_i$ in (1) and making the density of each section $\rho_i$ converge to a predefined value, denoted as $\rho^*$. In the ideal case ($\mu_i = 0$), a trivial choice is to let $\rho^* = C_b/v_f$, which corresponds to the highest possible flow-rate through the bottleneck. However, a small disturbance may drive the density towards the capacity-drop region, which introduces unwanted oscillatory behavior of the closed-loop system and negatively impacts convergence to desired equilibrium states [31]. On one hand, the value of $\rho^*$ needs to be compromised for the sake of robustness, i.e., $\rho^* < C_b/v_f$. On the other hand, it should be chosen so that the capacity is not reduced significantly.

When the VSL command of section $i$ ($v_i$) is activated, the maximum possible flow governed by $v_i$ is $\frac{v_i w \rho^j}{v_i + w}$, which is obtained by computing the coordinates of the geometric intersection of the supply and demand function in the fundamental diagram [30]. Therefore, the dynamics of the traffic flows when the VSL control is activated are described as follows:

$$
\begin{aligned}
q_1 &= \min\{d, \tfrac{v_0 w \rho^j}{v_0 + w}, \tfrac{v_1 w \rho^j}{v_1 + w}, w(\rho^j - \rho_1)\} \\
q_i &= \min\{v_{i-1}\rho_{i-1}, \tfrac{v_{i-1} w \rho^j}{v_{i-1} + w}, \tfrac{v_i w \rho^j}{v_i + w}, w(\rho^j - \rho_i)\} \qquad \text{for } i = 2, \dots, M-1, M+2, \dots, N \\
q_M &= \min\{v_{M-1}\rho_{M-1}, \tfrac{v_{M-1} w \rho^j}{v_{M-1} + w}, \tfrac{v_M w \rho^j}{v_M + w}, w\big(\rho^j - \rho_M\big), (1 - \epsilon(\rho_M))C_b\} \\
q_{M+1} &= \min\{v_M \rho_M, \tfrac{v_M w \rho^j}{v_M + w}, \tfrac{v_{M+1} w \rho^j}{v_{M+1} + w}, w\big(\rho^j - \rho_{M+1}\big), (1 - \epsilon(\rho_M))C_b\} \\
q_{N+1} &= \min\{v_N \rho_N, \widetilde{w}\big(\tilde{\rho}^j - \rho_N\big), (1 - \epsilon(\rho_N))C_d\}
\end{aligned}
\tag{3}
$$

Since the mainstream demand $d$ is the primary input of the freeway, the control efforts should be concentrated on the most upstream VSL section to ensure that $q_1$ is within the bottleneck capacity, and the goal for the remaining downstream sections is to maintain a steady traffic flow with the assistance from the RM control. The above strategy minimizes the speed variations between consecutive sections and diminishes the stop-and-go traffic behavior [11]. Driven by this idea, the VSL commands for each section can be computed as follows:

$$
v_{i-1} = \begin{cases} \frac{w q_1^v}{w\rho^j - q_1^v} & if\ i = 1 \\ \frac{q_i^v}{\rho_i} & if\ i = 2, \dots, M \\ v_f & otherwise \end{cases}
\tag{4}
$$

where $q_i^v$ is the desired mainstream inflow of section $i$. Assume that the disturbance $\mu_i$ in (1) is bounded by a constant $\mu_m$ and satisfies $|\mu_i| \leq \mu_m \ll C_b$. In order to reject $\mu_i$ and guarantee the convergence of the closed-loop system, we compute $q_i^v$ using the following proportional-integral (PI) controller equation [28, 31]:

$$q_i^v = q_{i+1} + s_i - r_i - \lambda_1(\rho_i - \rho^*) - \lambda_2\left(\int_{t_0}^{t}(\rho_i - \rho^*)d\tau - \frac{\lambda_1(\rho_i(t_0)-\rho^*)-\mu_m}{\lambda_2}\right) \quad (5)$$

where $q_{i+1}, \rho_i, s_i, r_i$ are measured traffic states, $\lambda_1 > 0$ and $\lambda_2 > 0$ are the proportional and integral gains to be tuned via simulations, $t_0$ denotes the time when the controller is activated.

The following constraints are applied to the computed VSL commands to improve safety and feasibility in real world:

- $v_i$ is rounded to be a multiple of 10 km/h.
- The bounds of $v_i$: 30 km/h $\leq v_i \leq$ 100 km/h.
- $v_i$ can be increased or decreased by at most 10 km/h in each control cycle.

The length of the most upstream VSL zone ($L_0$) has a significant impact on the VSL control performance [11]. $L_0$ needs to be long enough to prevent extra backpropagations from the bottleneck, but overextending $L_0$ may waste the road capacity and create unnecessary travel delays. In this project, we extend the lower bound of $L_0$ developed from our previous research by involving ramp flows and movable bottleneck locations:

***Theorem 1.*** Consider the freeway bottleneck control problem with VSL commands given by (4), the propagation of traffic congestion at the bottleneck can be completely dissipated if the upstream VSL zone distance $L_0$ satisfies

$$L_0 > \frac{(Q_r + v_f\bar{\rho}(t_0) - (1-\epsilon_0)C_b)v_0^* L_b}{((1-\epsilon_0)C_b - Q_r - v_0^*\rho_0(t_0))v_f} \quad (6)$$

where $\rho_0$ is the density of the upstream VSL section; $\bar{\rho}$ is the average density from section 1 to $M$; $L_b$ is the distance from the beginning of section 1 to the bottleneck; $C_b$ is the bottleneck capacity; $v_f$ is the free flow speed; $\epsilon_0$ is the capacity drop factor; $t_0$ is the time the incident takes place; $v_0^*$ is the value of $v_0$ that makes $q_1$ equal to $\rho^* v_f$:

$$v_0^* = \frac{w\rho^* v_f}{w\rho^j - \rho^* v_f} \quad (7)$$

$Q_r$ is the net flow of all ramps from section 1 to $M$:

$$Q_r = \sum_{i=1}^{M} r_i - s_i \quad (8)$$

***Proof.*** To fully dissipate the traffic congestion at the bottleneck and stop any further backpropagation, we must ensure that the time it takes to evacuate the initial traffic within the freeway network through the bottleneck, denoted as $T_{ini}$, is strictly less than the time spent for the newly-entered traffic to reach the bottleneck, denoted as $T_{new}$, under the impact of ramp flows.

To determine $T_{ini}$, we first estimate the number of vehicles $N_{ini}$ initially existing from the freeway entrance to the bottleneck using density measurements:

$$N_{ini} = L_0\rho_0(t_0) + L_b\bar{\rho}(t_0) \tag{9}$$

Since the congestion is active at the bottleneck, the bottleneck throughput is $q_b = (1-\epsilon_0)C_b$ due to the capacity drop. Assuming the bottleneck throughput $q_b$ and the net ramp flow $Q_r$ are constants during the congestion resolving process, $T_{ini}$ is computed as follows:

$$T_{ini} = \frac{N_{ini}}{q_b - Q_r} = \frac{L_0\rho_0(t_0)+L_b\bar{\rho}(t_0)}{(1-\epsilon_0)C_b - Q_r} \tag{10}$$

On the other hand, the newly-entered traffic travel through the network under the activated VSL commands. The proposed VSL control strategy matches $q_1$ with the selected equilibrium $\rho^* v_f$ using $v_0^*$ in the most upstream section, and then maintains a steady traffic flow through downstream sections with speed limits ideally equal to $v_f$. Therefore, $T_{new}$ can be estimated as

$$T_{new} = \frac{L_0}{v_0^*} + \frac{L_b}{v_f} \tag{11}$$

To guarantee $T_{ini} < T_{new}$, we have

$$\frac{L_0\rho_0(t_0)+L_b\bar{\rho}(t_0)}{(1-\epsilon_0)C_b - Q_r} < \frac{L_0}{v_0^*} + \frac{L_b}{v_f} \tag{12}$$

which is equivalent to (6) after rearranging the above inequality and keeping $L_0$ only on the left side.

### *Lane Change Control*

To mitigate the capacity drop triggered by forced lane change maneuvers and increase the throughput at the bottleneck, we provide lane change (LC) recommendations to vehicles moving in the closed lane(s) before approaching the bottleneck. The distance from the bottleneck to activate the LC control, denoted as $d_{LC}$, is a crucial control variable that needs to be determined properly. $d_{LC}$ must be longer than the minimum distance required for vehicles to complete LC maneuvers safely, but overextending $d_{LC}$ may lead to the underutilization of the road capacity. In this project, $d_{LC}$ is computed from the empirical formula proposed in [15]:

$$d_{LC} = \xi \cdot n \tag{13}$$

where $n$ is the number of lanes closed at the bottleneck, $\xi$ is a design parameter that depends on the traffic demand and can be found via microscopic simulations.

### *Ramp Metering*

As mentioned previously, the performance of VSL control in regulating the traffic flow relies on a steady ramp input within the mainstream receiving ability, which is achieved by the ramp metering (RM) control. In the meantime, the ramp queue should not exceed the length of the ramp. Therefore, the RM controller needs to maintain a good balance between the mainstream traffic and the ramp queue. A well-known solution to the above problem is the ALINEA/Q

algorithm proposed in [17] - an extension of the classic ALINEA algorithm by considering the ramp queue capacity. Note that the original ALINEA/Q contains both the occupancy and the queue length in the feedback loop. In this project, we use the density of the mainstream section instead of the occupancy in order to be consistent with the mechanism of the VSL control [64].

The adopted ALINEA/Q algorithm involves 3 steps in general:

1) Compute the first RM rate $r_i^d$ based on the mainstream density $\rho_i$ and the RM rate of previous control cycle.
2) Compute the second RM rate $r_i^q$ based on the queue length $w_i$ and the estimated demand $\tilde{d}_i$ for the on-ramp at CTM section $i$.
3) Take the maximum between $r_i^d$ and $r_i^q$ as the final RM rate $r_i$.

which is expressed by the following equations:

$$\begin{aligned} r_i^d(t) &= r_i(t-T) + \beta_d(\rho^* - \rho_i(t)) \\ r_i^q(t) &= \beta_q\left(w_i^r - w_i(t)\right) + \tilde{d}_i \\ r_i(t) &= \max\{r_i^d(t), r_i^q(t)\} \end{aligned} \tag{14}$$

where $t$ is the current time, $T$ is the control cycle, $\rho^*$ is the desired density, $w_i^r$ is the reference queue capacity of ramp $i$, $\beta_d$ and $\beta_q$ are the feedback gains of the density and queue length respectively. The estimation process of $\tilde{d}_i$ is presented later using the arterial traffic states and signal plans.

Although the RM algorithm is able to prevent the spillback of the ramp queue to some extent, the effect would be limited when the freeway is heavily occupied and meanwhile there exist large on-ramp demands, which happens frequently during peak hours in the urban area of major cities. In this case, the assistance from arterial traffic management is needed to exploit the capacity of potentially unsaturated arterial roads and evenly distribute the loads of all available ramps.

## Arterial Traffic Management

The arterial road network under consideration contains $K$ homogeneous signalized intersections indexed from $1$ to $K$ in the freeway traffic flow direction, as depicted in Figure 1. The on-ramp entrances and off-ramp exits lie on the East side of each intersection. There are $2(K+1)$ entrances plus $N$ off-ramps that generate traffic flow into the arterial road network. Some of these inputs may exceed the road or ramp capacity, leading to heavy congestion and long queues at corresponding locations. Incidents or road constructions may worsen the situation as they introduce bottlenecks that lower the capacity. At this stage, we assume traffic signal control (TSC) is the only method to regulate arterial traffic flows. Fixed-time TSC strategies cannot fit various input levels and traffic conditions as mentioned in the literature review. Therefore, we propose a traffic-responsive scheme to determine the optimal signal

program that minimizes the travel time, the fuel consumption and the emissions for each intersection based on the observation of input demands, which consists of two main steps:

1) Compute a modified Webster cycle length model for isolated intersections.
2) Apply the model for each intersection in the original arterial network with estimated demands.

### *Cycle Length Model*

The pioneer research on signal cycle optimization was conducted by F. V. Webster [46, 47], who developed a formula to compute the signal cycle that minimizes travel delays while considering the uncertainties of traffic models as follows:

$$T_c^* = \frac{1.5T_l+5}{1-Y} \tag{15}$$

where $T_c$ is the signal cycle and $T_l$ is the lost time per cycle. The lost time is defined as the time during which no vehicles are able to pass through an intersection due to the transition between a green phase and a red phase. $Y \in [0, 1)$ is the sum of flow ratios of each phase group, which indicates the degree of saturation of an intersection. The flow ratio is defined as the actual traffic flow divided by the saturation flow. The saturation flow is set to be 1800 veh/h/lane in this project. Extensions based on the Webster model have been made over the years to optimize different objective functions such as fuel consumption, emissions and the number of vehicle stops [65-67]. In this paper, we adopt the modified Webster model proposed by Calle-Laguna et al. [67]:

$$T_c^* = \alpha_1 \ln\left(\frac{T_l}{1-Y}\right) + \alpha_2 \tag{16}$$

where $\alpha_1$ and $\alpha_2$ are determined by solving a linear regression problem on the data collected from microscopic simulations over an isolated intersection. The detailed configuration of the isolated intersection is presented in Figure 3. Each intersection is four lanes wide (left, right, and a double through) with a length of 100 m. The arterial road connected to the intersection is two lanes wide and lasts for 1 km on each direction in order to accommodate the long queue under high demands. The default signal plan involves four phases as shown in Figure 4. Since only medium and high traffic demands are considered, all signal plans must have a separate left-turn phase to enhance the mobility and safety of the intersection operation [68].

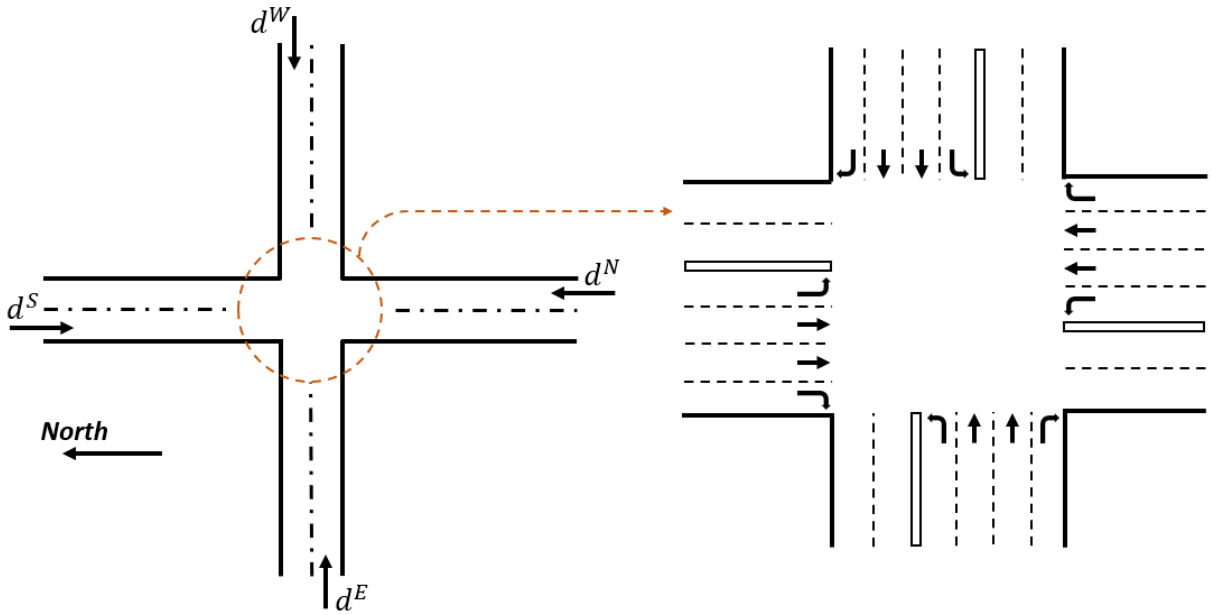


**Figure 3. Intersection configuration**

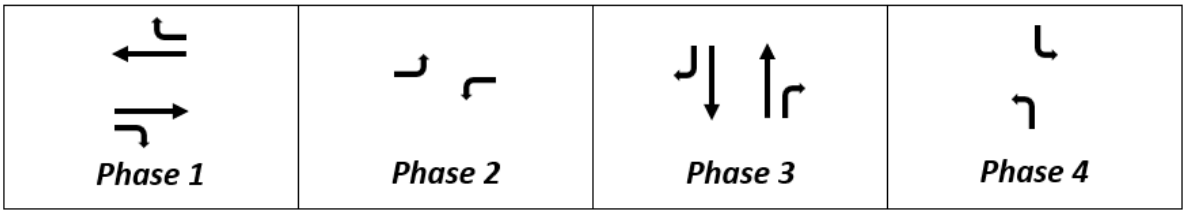


**Figure 4. Signal phasing scheme**

The commercial microscopic simulator PTV VISSIM 10 is used to generate the data for estimating the model parameters $\alpha_1$ and $\alpha_2$ in (16). The vehicle inputs are set to be equal for all directions ($d^W = d^N = d^E = d^S$) and selected from 500 to 2000 veh/h with the increment of 50 veh/h. For each input level, we test a wide range of signal cycles from 30 to 180 s with the increment of 10 s, and evaluate their performance using the following performance index function [65]:

$$P = \gamma_1 \frac{T_t}{T_{t,0}} + \gamma_2 \frac{F}{F_0} + \gamma_3 \frac{E}{E_0} \tag{17}$$

where $T_t$ is the average travel time, $F$ is the average fuel consumption, $E$ is the average emission rates of $CO_2$, and $\gamma_1, \gamma_2, \gamma_3$ are the corresponding weights. $F$ and $E$ are computed using the EPA MOVES model [69]. $T_{t,0}, F_0, E_0$ are the base-case results obtained from the scenario where the signal cycle is 60 s. According to [65], we set $\gamma_1 = 0.4, \gamma_2 = \gamma_3 = 0.3$. The lost time $T_l$ is 16 s per cycle. The turning ratio of each approach is 20% left-turn traffic, 60% through traffic and 20% right-turn traffic. The data collection process is summarized as follows:

1) Set the vehicle input for each entrance.

2) Compute the flow ratio with respect to the saturation flow for each phase group.
3) Repeat the simulation for each signal cycle:
    a. Set the signal cycle and allocate the green light time according to the flow ratio of each phase.
    b. Run the simulation for 30 min.
    c. Compute the performance index using (17).
4) Find the cycle length that yields the lowest performance index.

After iterating the above process for all input levels twice, we plot the obtained data points and the linear regression curve in Figure 5. As a result, $\alpha_1 = 76.9$ and $\alpha_2 = -186.2$.

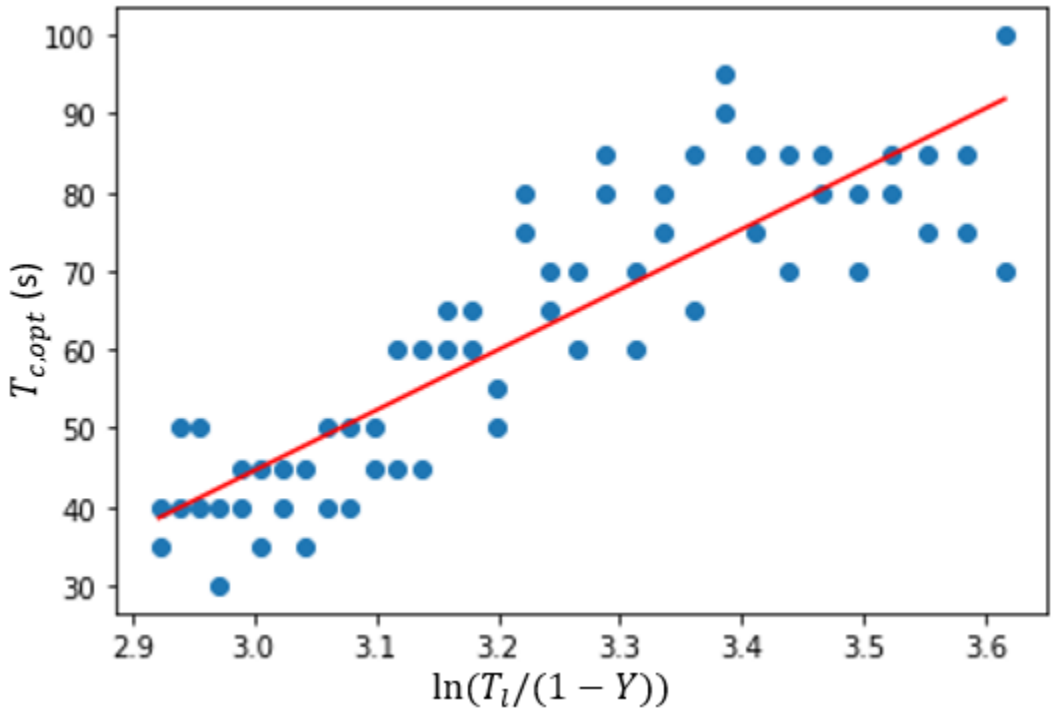


**Figure 5. Determine cycle length model using linear regression**

### *Model Application*

Since the intersections in the interested road network have a uniform configuration identical to the one presented in Figure 3, the derived optimal cycle length model is applicable to all the intersections. If there exist intersections with different configurations, separate models need to be computed using the same approach presented above. To apply the model, we first estimate the demands of each intersection as follows:

$$\tilde{d}_k^W = d_k^W + s_i$$
$$\tilde{d}_k^E = d_k^E$$

$$\tilde{d}_k^S = \begin{cases} d_1^S & \text{if } k = 1 \\ y_{k-1}^{W,l}\tilde{d}_{k-1}^W + y_{k-1}^{E,r}\tilde{d}_{k-1}^E + y_{k-1}^{S,t}\tilde{d}_{k-1}^S & \text{otherwise} \end{cases}$$

$$\tilde{d}_k^N = \begin{cases} d_K^N & \text{if } k = K \\ y_{k+1}^{W,r}\tilde{d}_{k+1}^W + y_{k+1}^{E,l}\tilde{d}_{k+1}^E + y_{k+1}^{N,t}\tilde{d}_{k+1}^N & \text{otherwise} \end{cases} \quad (18)$$

where $\tilde{d}_k^W$ is the estimated demand of the Westbound approach at intersection $k$, $d_k^W$ is the actual Westbound vehicle input of intersection $k$, $s_i$ is the off-ramp flow rate heading toward intersection $k$ ($s_i = 0$ if the off-ramp does not exist), $y_k^{W,l}$ is the left-turn flow ratio of the Westbound approach at intersection $k$. The superscript denotes the traffic flow direction in the following manner: $E$ - Eastbound, $W$ - Westbound, $N$ - Northbound, $S$ - Southbound, $l$ - left-turn, $r$ - right-turn, $t$ - through. We assume all vehicle inputs and turning ratios are known with uncertainties and all links within the arterial network are unsaturated.

Based on the estimated demands, we calculate the flow ratio of each phase group with respect to the phase scheme presented in Figure 4 and sum them up to obtain $Y$:

$$\begin{aligned} Y_1 &= \frac{(y^{S,r}+y^{S,t})\tilde{d}^S}{q_s^S} + \frac{(y^{N,r}+y^{N,t})\tilde{d}^N}{q_s^N} \\ Y_2 &= \frac{y^{S,l}\tilde{d}^S}{q_s^S} + \frac{y^{N,l}\tilde{d}^N}{q_s^N} \\ Y_3 &= \frac{(y^{W,r}+y^{W,t})\tilde{d}^W}{q_s^W} + \frac{(y^{E,r}+y^{E,t})\tilde{d}^E}{q_s^E} \\ Y_4 &= \frac{y^{W,l}\tilde{d}^W}{q_s^W} + \frac{y^{E,l}\tilde{d}^E}{q_s^E} \\ Y &= Y_1 + Y_2 + Y_3 + Y_4 \end{aligned} \quad (19)$$

where $q_s$ is the saturation flow of the approach whose direction is specified by the superscript. In this project, $q_s = 7200$ veh/h for all directions at each intersection. Since (19) applies to all intersections in the road network, the index of the intersection is omitted for the sake of simplicity.

We then compute the cycle length $T_c$ for each intersection using (16) with the following feasibility constraints:

- $T_c$ is rounded to be a multiple of 10 s.
- 30 s $\leq T_c \leq$ 180 s.

Once $T_c$ is determined, we can allocate the green light time for each phase according to the flow ratios found in (19):

$$T_{g,j} = \frac{(T_c - T_l)Y_j}{Y} \qquad \text{for } j = 1, 2, 3, 4 \quad (20)$$

where $T_{g,j}$ denotes the green light time of phase $j$ per cycle, and the lost time $T_l = 16$ s.

To minimize travel delays and improve the traffic mobility, it is recommended to unify the cycle length for closely spaced traffic signal and use proper offsets to create a progression band

(green wave) for vehicle platoons on the main street [68]. However, the intersections in our simulation network are relatively far apart with a minimum distance of 600 m and 1500 m on average. Besides, the longitudinal traffic is not significantly larger than the lateral traffic at each intersection. Therefore, the offset optimization is not considered in this project. The offset of each signal is simply set to 0 s.

### *On-ramp Demand Estimation*

As previously mentioned, the on-ramp demand estimation must be as accurate as possible for the adopted ramp metering (RM) algorithm to be effective. Assuming the arterial road linked with on-ramp $i$ is also connected to intersection $k$, we estimate the on-ramp demand using the knowledge of the arterial signal plans as follows:

$$\tilde{d}_i = \frac{y_i^{on}(T_{g,1}\tilde{d}_k^N + T_{g,2}\tilde{d}_k^S + T_{g,3}\tilde{d}_k^E)}{T_c} \tag{21}$$

where the green light time $T_{g,j}$ and the cycle length $T_c$ are associated with intersection $k$. $y_i^{on}$ is the $i$-th on-ramp turning ratio.

## Numerical Simulations

### Simulation Network

The proposed control methodologies are simulated using a microscopic traffic simulator based on the commercial software PTV Vissim 10. The road network in Figure 6 contains a 16-km segment of I-710 freeway and the adjacent arterial region in Los Angeles, California, United States. The freeway segment is divided into 6 CTM sections and one upstream VSL zone. Each CTM section has a length of 2 km. The length of the upstream VSL zone is determined by (6). The freeway segment has 5 lanes, 5 on-ramps and 5 off-ramps. All ramps are connected with the arterial road network. There are 7 arterial intersections aligned in parallel with the freeway. Vehicle inputs are generated from one freeway entrance and 16 arterial entrances as indicated by arrows in Figure 6. The left and right turning ratio of each approach follows the normal distribution $N(0.2, 0.02)$, and the through traffic ratio follows $N(0.6, 0.06)$, if not specified otherwise. The default on-ramp turning ratio follows $N(0.7, 0.07)$, and the default off-ramp turning ratio follows $N(0.4, 0.04)$. The mean values of these turning ratio distributions are calculated based on the traffic data of April 2019 from PeMS. Each vehicle input of the network also follows a normal distribution whose mean value is obtained from the same data source, and the standard deviation is set to be 10% of the mean. Each simulation run lasts for 40 min. The incident takes place after a 10-min warm up and will be cleared at 30 min.

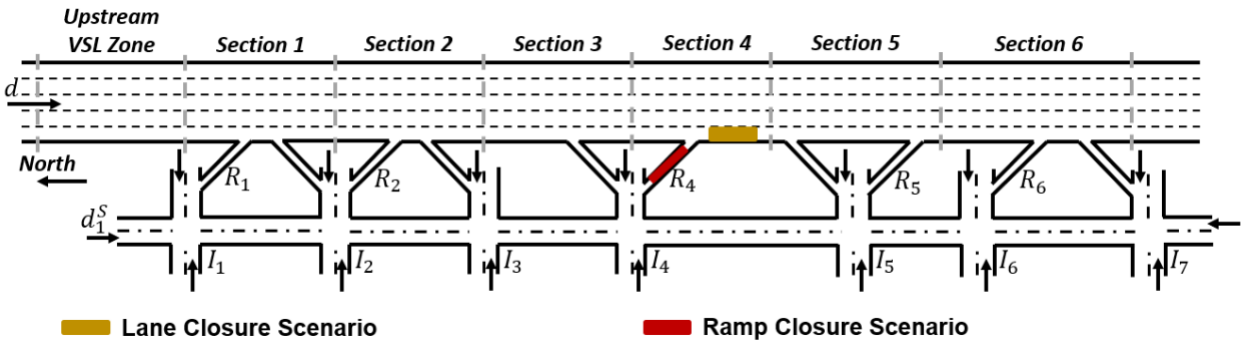


**Figure 6. Simulation road network**

## No Incident Scenario

In this section, we present the simulation results without any incident in the road network in Figure 6. The vehicle inputs are in a moderate level, therefore no significant congestion is produced in this scenario. The active controllers are ramp metering and arterial traffic signal control. To quantify the benefits by coordinating ramp metering (RM) with adjacent arterial traffic signal control (TSC), we compare the performance of two types of control strategies – without coordination (denoted as type (i)) and with coordination (denoted as type (ii)). To be more specific, in type (i) control, the RM controller cannot estimate the demand using (21), which is replaced by the RM rate of the previous cycle. The TSC has no information of the off-ramp flow rate, instead it uses the historical average value.

The evaluation standard involves the average travel time ($T_t$), the average number of stops ($N_s$) and the average emission rates of $CO_2$ ($E$). To simplify the notation, we use $I_j$ to denote the $j$-th intersection where $j = 1, 2, \dots, 7$ and $R_i$ to denote each on-ramp where $i$ is the index of the corresponding CTM section. $T_t, N_s, E$ are evaluated for both freeway and arterial separately. The details of computing $T_t, N_s, E$ can be found in [15]. Considering the stochastic nature of microscopic simulations, we take the average of 10 simulation runs for each case and record the final results in Table 2.

**Table 2. Evaluations of no incident scenario**

| Region | Control Type | $T_t$ (min) | $N_s$ | $E$ (g/veh/km) |
|---|---|---|---|---|
| Freeway | (i) | 10.2 | 0.1 | 202.8 |
| Freeway | (ii) | 10.2 | 0.1 | 204.6 |
| Arterial | (i) | 4.0 | 1.3 | 230.6 |
| Arterial | (ii) | 3.8 | 1.2 | 229.1 |

As we compare the evaluation results of control (i) and (ii), the improvement produced by (ii) over (i) is trivial in this scenario, which indicates that the coordination between RM and TSC cannot produce much benefit under free flow conditions. In the next two scenarios, we will introduce some incidents to break the free flow condition and reexamine the effectiveness of the proposed coordination strategy.

## Ramp Closure Scenario

In this section, we present the simulation results in a ramp closure scenario marked by the red rectangle in Figure 6. Assuming most vehicles reroute to the next available on-ramp during the incident, we change the mean values of the turning ratio distributions (left-turn/through/right-turn) at critical approaches as follows:

- Eastbound approach at intersection 4: 0.2/0.2/0.6
- Southbound approach at intersection 4: 0.1/0.7/0.2
- Southbound approach at intersection 5: 0.5/0.4/0.1

The standard deviation remains to be 10% of the mean.

Since the freeway is not blocked by the incident, VSL and LC control are inactive in this scenario. We are interested in the performance of three types of control strategies as follows:

(i) Inactive ramp metering
(ii) No coordination between RM and TSC
(iii) Coordinated RM and TSC

In the first control strategy, the on-ramp metering is inactive, thus there is no restriction for on-ramp travel. In the second control strategy, the RM controller cannot estimate the demand using (21), instead it is replaced by the RM rate of the previous cycle. In both the above strategies, the TSC does not know the off-ramp flow rate, instead it uses the historical average value when computing signal plans. Table 3 presents the evaluation results for the ramp closure scenario.

**Table 3. Evaluations of ramp closure scenario**

| Region | Control Type | $T_t$ (min) | $N_s$ | $E$ (g/veh/km) |
|---|---|---|---|---|
| Freeway | (i) | 10.2 | 0.1 | 202.2 |
| Freeway | (ii) | 10.2 | 0.1 | 202.7 |
| Freeway | (iii) | 9.9 | 0.1 | 198.8 |
| Arterial | (i) | 4.9 | 1.4 | 250.6 |
| Arterial | (ii) | 4.8 | 1.2 | 248.5 |
| Arterial | (iii) | 4.5 | 1.2 | 236.7 |

In Table 3, the proposed ramp metering algorithm cannot provide much benefit without knowing the incoming demand as we compare the freeway results of control (i) and (ii). With estimated demand, the RM improves the freeway travel time by 3% and the emission of $CO_2$ by 2%. The proposed TSC also requires the knowledge of off-ramp flow rate to compute proper signal plans. As we compare the arterial results of control (ii) and (iii), the coordination improves the travel time by 6% and the emission of $CO_2$ by 5%. These evaluation results indicate that the data-sharing mechanism between ramp metering and arterial intersections is beneficial to the control efficiency of both sides.

## Lane Closure Scenario

In this section, we test the proposed integrated control strategy in a freeway lane closure scenario marked by the gold rectangle in Figure 6. The incident takes place at 30 m downstream the freeway merging point of the on-ramp $R_4$, which creates a bottleneck at CTM section 4 ($M = 4$) and congestion at $R_4$ by hindering the merging process. Assuming the ramp congestion at $R_4$ makes some vehicles reroute to $R_5$ during the incident, we change the mean values of the turning ratio distributions (left-turn/through/right-turn) at critical approaches as follows:

- Eastbound approach at intersection 4: 0.2/0.4/0.4
- Southbound approach at intersection 4: 0.15/0.65/0.2
- Southbound approach at intersection 5: 0.4/0.4/0.2

The standard deviation remains to be 10% of the mean.

To identify the benefits provided by each control component as well as the coordination, we compare the performance of three types of control strategies as follows:

(i) Inactive freeway control
(ii) No coordination between freeway and arterials
(iii) Proposed integrated control

In the first control strategy, VSL, LC and RM are inactive despite the existence of the freeway bottleneck. In the second control strategy, the VSL control has no ramp flow information, thus, $s_i$ and $r_i$ are ignored when computing the desired CTM inflow using (5). The restrictions on RM and TSC are the same as the second control strategy in the ramp closure scenario.

Table 4 presents the evaluation results for the lane closure scenario.

**Table 4. Evaluations of lane closure scenario**

| Region | Control Type | $T_t$ (min) | $N_s$ | $E$ (g/veh/km) |
|---|---|---|---|---|
| Freeway | (i) | 12.9 | 1.2 | 215.7 |
| Freeway | (ii) | 11.7 | 0.3 | 215.5 |
| Freeway | (iii) | 10.9 | 0.3 | 208.2 |
| Arterial | (i) | 5.1 | 2.0 | 251.9 |
| Arterial | (ii) | 4.9 | 1.3 | 244.3 |
| Arterial | (iii) | 4.4 | 1.2 | 234.0 |

The effectiveness of the proposed freeway control on a lane-drop bottleneck is verified by comparing the freeway results of (i) and (ii). However, without the knowledge of ramp flow and on-ramp demand, the efficiency of VSL and RM is suboptimal. The freeway travel time and the emission of CO2 can be further reduced by 7% and 3.5% with the proposed data-sharing mechanism. The dissipation of freeway bottleneck congestion allows more on-ramp traffic to get through and slightly improves the arterial traffic mobility as we compare the arterial results of (i) and (ii). With the knowledge of off-ramp flows as part of the TSC input, the arterial travel

time and the emission of CO2 are reduced by 10% and 4%. These evaluation results verify the significance of coordination in terms of both freeway and arterial traffic control.

### Sensitivity of Turning Ratios

In this section, we discuss how sensitive the system is with respect to turning ratios. As mentioned previously, the turning ratio follows a normal distribution, and thus, it changes slightly in each simulation run under the same case. The evaluation results under the same case in terms of $T_t, N_s, E$ are mostly within a 5% range of the average value, which indicates that the proposed approach is robust against small disturbances in turning ratios. However, if the turning ratios change dramatically due to the incidents, we observe 10-25% increase in arterial travel time depending on the types of control. Note that the incidents are not located in arterials and the arterial congestion is triggered by the changes of turning ratios. Therefore, the results imply that the proposed approach cannot perfectly handle such dramatic changes of turning ratios.

## Conclusion

In this project, we proposed an integrated freeway and arterial traffic management strategy to improve the operation efficiency of both systems under various traffic conditions. The freeway part consists of a robust VSL controller to maintain a steady traffic flow around the desired value, an LC controller to reduce the capacity drop at a lane-drop bottleneck, and an RM algorithm to balance the mainstream density and the ramp queue. The on-ramp demand is estimated using the signal plan of the adjacent arterial intersection when computing the RM rate. The arterial signal plans are determined by simulation-based cycle length models and estimated demands of all intersection approaches in a traffic-responsive manner. Sharing measurements and control plans between the two systems improves the accuracy of traffic state estimations, and thus, enhances the overall control performance. We tested the proposed approach on a segment of I-710 freeway along with the adjacent arterial intersections using microscopic simulations. As a result, the coordinated control does not produce significant benefit over individual control in the free flow scenario without incidents. However, when the on-ramp or freeway lane is blocked by an incident, the coordination improves the average travel time and the emission rate of CO2 for the specific region affected by the incident. In the lane closure scenario, both freeway and arterial traffic control achieve higher operation efficiency when using the proposed coordination strategy.

## References


[1] R. C. Carlson, I. Papamichail, M. Papageorgiou, and A. Messmer, “Optimal motorway traffic flow control involving variable speed limits and ramp metering,” Transportation science, vol. 44, no. 2, pp. 238–253, 2010.

[2] Y. Zhang and P. A. Ioannou, “Integrated control of highway traffic flow,” Journal of Control and Decision, vol. 5, no. 1, pp. 19–41, 2018.

[3] J. R. D. Frejo and B. De Schutter, “Logic-based traffic flow control for ramp metering and variable speed limits—part 1: Controller,” IEEE Transactions on Intelligent Transportation Systems, vol. 22, no. 5, pp. 2647–2657, 2020.

[4] G. De Nunzio, G. Gomes, C. Canudas-de Wit, R. Horowitz, and P. Moulin, “Speed advisory and signal offsets control for arterial bandwidth maximization and energy consumption reduction,” IEEE Transactions on Control Systems Technology, vol. 25, no. 3, pp. 875–887, 2016.

[5] P. Wang, Y. Jiang, L. Xiao, Y. Zhao, and Y. Li, “A joint control model for connected vehicle platoon and arterial signal coordination,” Journal of Intelligent Transportation Systems, vol. 24, no. 1, pp. 81–92, 2020.

[6] H. Wang and X. Peng, “Coordinated control model for oversaturated arterial intersections,” IEEE Transactions on Intelligent Transportation Systems, vol. 23, no. 12, pp.24157-24175, 2022.

[7] T. Urbanik, D. Humphreys, B. Smith, S. Levine et al., “Coordinated freeway and arterial operations handbook,” United States. Federal Highway Administration, Tech. Rep., 2006.

[8] Q. Yang, H. Wei, and J. Gu, “Linking freeway and arterial data-data archiving testing in supporting coordinated freeway and arterial operations,” in 2008 11th International IEEE Conference on Intelligent Transportation Systems. IEEE, 2008, pp. 259–264.

[9] D. Su, X.-Y. Lu, R. Horowitz, and Z. Wang, “Coordinated ramp metering and intersection signal control,” International Journal of Transportation Science and Technology, vol. 3, no. 2, pp. 179–192, 2014.

[10] J. C. Aydos and A. O’Brien, “Scats ramp metering: strategies, arterial integration and results,” in 17th international IEEE conference on intelligent transportation systems (ITSC). IEEE, 2014, pp. 2194–2201.

[11] T. Yuan, F. Alasiri, and P. A. Ioannou, “Selection of the speed command distance for improved performance of a rule-based VSL and lane change control,” IEEE Transactions on Intelligent Transportation Systems, vol. 23, no. 10, pp.19348-19357, 2022.

[12] E. Kwon, D. Brannan, K. Shouman, C. Isackson, and B. Arseneau, “Development and field evaluation of variable advisory speed limit system for work zones,” Transportation research record, vol. 2015, no. 1, pp. 12–18, 2007.

[13] J. M. Torn´e Santos, D. M. Rosas D´ıaz, and F. Soriguera Mart´ı, “Evaluation of speed limit management on c-32 highway access to barcelona,” in Proceedings of the TRB 90th Annual Meeting, 2011, pp. 1–23.

[14] M. Hadiuzzaman and T. Z. Qiu, “Cell transmission model based variable speed limit control for freeways,” Canadian Journal of Civil Engineering, vol. 40, no. 1, pp. 46–56, 2013.

[15] Y. Zhang and P. A. Ioannou, “Combined variable speed limit and lane change control for highway traffic,” IEEE Transactions on Intelligent Transportation Systems, vol. 18, no. 7, pp. 1812–1823, 2017.

[16] M. Papageorgiou, H. Hadj-Salem, J.-M. Blosseville et al., “Alinea: A local feedback control law for on-ramp metering,” Transportation Research Record, vol. 1320, no. 1, pp. 58–67, 1991.

[17] E. Smaragdis and M. Papageorgiou, “Series of new local ramp metering strategies: Emmanouil smaragdis and markos papageorgiou,” Transportation Research Record, vol. 1856, no. 1, pp. 74–86, 2003.

[18] Y. Wang and M. Papageorgiou, “Local ramp metering in the case of distant downstream bottlenecks,” in 2006 IEEE Intelligent Transportation Systems Conference. IEEE, 2006, pp. 426–431.

[19] K. Shaaban, M. A. Khan, I. Kim, and R. Hamila, “Queue discharge at freeway on-ramps using coordinated operation of a ramp meter and an upstream traffic signal,” Procedia Computer Science, vol. 170, pp. 347–353, 2020.

[20] S. Smulders, “Control of freeway traffic flow by variable speed signs,” Transportation Research Part B: Methodological, vol. 24, no. 2, pp. 111–132, 1990.

[21] H. Zackor, “Speed limitation on freeways: Traffic-responsive strategies,” in Concise Encyclopedia of Traffic & Transportation Systems. Elsevier, 1991, pp. 507–511.

[22] A. Hegyi, B. De Schutter, and J. Heelendoorn, “MPC-based optimal coordination of variable speed limits to suppress shock waves in freeway traffic,” in Proceedings of the 2003 American Control Conference, vol. 5, pp. 4083–4088, 2003.

[23] J. R. D. Frejo, A. N´u˜nez, B. De Schutter, and E. F. Camacho, “Hybrid model predictive control for freeway traffic using discrete speed limit signals,” Transportation Research Part C: Emerging Technologies, vol. 46, pp. 309–325, 2014.

[24] B. Khondaker and L. Kattan, “Variable speed limit: A microscopic analysis in a connected vehicle environment,” Transportation Research Part C: Emerging Technologies, vol. 58, pp. 146–159, 2015.

[25] A. Muralidharan and R. Horowitz, “Computationally efficient model predictive control of freeway networks,” Transportation Research Part C: Emerging Technologies, vol. 58, pp. 532–553, 2015.

[26] R. C. Carlson, I. Papamichail, and M. Papageorgiou, “Comparison of local feedback controllers for the mainstream traffic flow on freeways using variable speed limits,” Journal of Intelligent Transportation Systems, vol. 17, no. 4, pp. 268–281, 2013.

[27] G.-R. Iordanidou, C. Roncoli, I. Papamichail, and M. Papageorgiou, “Feedback-based mainstream traffic flow control for multiple bottlenecks on motorways,” IEEE Transactions on Intelligent Transportation Systems, vol. 16, no. 2, pp. 610–621, 2014.

[28] H.-Y. Jin and W.-L. Jin, “Control of a lane-drop bottleneck through variable speed limits,” Transportation Research Part C: Emerging Technologies, vol. 58, pp. 568–584, 2015.

[29] Y. Zhang and P. A. Ioannou, “Stability analysis and variable speed limit control of a traffic flow model,” Transportation Research Part B: Methodological, vol. 118, pp. 31–65, 2018.

[30] T. Yuan, F. Alasiri, Y. Zhang, and P. A. Ioannou, “Evaluation of integrated variable speed limit and lane change control for highway traffic flow,” IFAC-PapersOnLine, vol. 54, no. 2, pp. 107–113, 2021.

[31] F. Alasiri, Y. Zhang, and P. A. Ioannou, “Robust variable speed limit control with respect to uncertainties,” European Journal of Control, 2020.

[32] M. Seraj, X. Wang, M. Hadiuzzaman, and T. Z. Qiu, “Optimal location identification of VSL signs for recurrent bottlenecks,” Transp. Res. Rec. J. Transp. Res. Board, vol. 82, no. 4, pp. 1084–1090, 2016.

[33] C. Xu, Z. Li, Z. Pu, Y. Guo, and P. Liu, “Procedure for determining the deployment locations of variable speed limit signs to reduce crash risks at freeway recurrent bottlenecks,” IEEE Access, vol. 7, pp. 47856–47863, 2019.

[34] I. Mart´ınez and W.-L. Jin, “Optimal location problem for variable speed limit application areas,” Transportation Research Part B: Methodological, vol. 138, pp. 221–246, 2020.

[35] Y. J. Stephanedes, “Implementation of on-line zone control strategies for optimal ramp metering in the minneapolis ring road,” 1994.

[36] H. M. Zhang and S. G. Ritchie, “Freeway ramp metering using artificial neural networks,” Transportation Research Part C: Emerging Technologies, vol. 5, no. 5, pp. 273–286, 1997.

[37] G. Paesani, J. Kerr, P. Perovich, and F. Khosravi, “System wide adaptive ramp metering (swarm),” in Merging the Transportation and Communications Revolutions. Abstracts for ITS America Seventh Annual Meetingand ExpositionITS America, 1997.

[38] I. Papamichail, M. Papageorgiou, V. Vong, and J. Gaffney, “Heuristic ramp-metering coordination strategy implemented at monash freeway, Australia,” Transportation Research Record, vol. 2178, no. 1, pp. 10–20, 2010.

[39] Y. Han, M. Ramezani, A. Hegyi, Y. Yuan, and S. Hoogendoorn, “Hierarchical ramp metering in freeways: an aggregated modeling and control approach,” Transportation research part C: emerging technologies, vol. 110, pp. 1–19, 2020.

[40] A. Hegyi, B. De Schutter, and H. Hellendoorn, “Model predictive control for optimal coordination of ramp metering and variable speed limits,” Transportation Research Part C: Emerging Technologies, vol. 13, no. 3, pp. 185–209, 2005.

[41] A. H. Ghods, A. R. Kian, and M. Tabibi, “Adaptive freeway ramp metering and variable speed limit control: a genetic-fuzzy approach,” IEEE Intelligent Transportation Systems Magazine, vol. 1, no. 1, pp. 27–36, 2009.

[42] J. R. D. Frejo and E. F. Camacho, “Global versus local MPC algorithms in freeway traffic control with ramp metering and variable speed limits,” IEEE Transactions on intelligent transportation systems, vol. 13, no. 4, pp. 1556–1565, 2012.

[43] C. Pasquale, S. Sacone, S. Siri, and B. De Schutter, “A multi-class model-based control scheme for reducing congestion and emissions in freeway networks by combining ramp metering and route guidance,” Transportation Research Part C: Emerging Technologies, vol. 80, pp. 384–408, 2017.

[44] I. Schelling, A. Hegyi, and S. P. Hoogendoorn, “Specialistrm—integrated variable speed limit control and ramp metering based on shock wave theory,” in 2011 14th International IEEE conference on intelligent transportation systems (ITSC). IEEE, 2011, pp. 2154–2159.

[45] G. R. Iordanidou, I. Papamichail, C. Roncoli, and M. Papageorgiou, “Feedback-based integrated motorway traffic flow control with delay balancing,” IEEE Transactions on Intelligent Transportation Systems, vol. 18, no. 9, pp. 2319–2329, 2017.

[46] F. V. Webster, “Traffic signal settings,” Tech. Rep., 1958.

[47] F. Webster, “Traffic signals,” Road research technical paper, vol. 56, 1966.

[48] J. D. Little, M. D. Kelson, and N. H. Gartner, “Maxband: A versatile program for setting signals on arteries and triangular networks,” 1981.

[49] D. I. Robertson, “‘tansyt’method for area traffic control,” Traffic Engineering & Control, vol. 8, no. 8, 1969.

[50] N. H. Gartner, S. F. Assman, F. Lasaga, and D. L. Hou, “A multi-band approach to arterial traffic signal optimization,” Transportation Research Part B: Methodological, vol. 25, no. 1, pp. 55–74, 1991.

[51] T. Arsava, Y. Xie, and N. H. Gartner, “Arterial progression optimization using od-band: case study and extensions,” Transportation Research Record, vol. 2558, no. 1, pp. 1–10, 2016.

[52] P. Hunt, D. Robertson, R. Bretherton, and M. C. Royle, “The scoot on-line traffic signal optimisation technique,” Traffic Engineering & Control, vol. 23, no. 4, 1982.

[53] P. Mirchandani and F.-Y. Wang, “Rhodes to intelligent transportation systems,” IEEE Intelligent Systems, vol. 20, no. 1, pp. 10–15, 2005.

[54] M. Van den Berg, A. Hegyi, B. De Schutter, and H. Hellendoorn, “Integrated traffic control for mixed urban and freeway networks: A model predictive control approach,” European journal of transport and infrastructure research, vol. 7, no. 3, 2007.

[55] J. Haddad, M. Ramezani, and N. Geroliminis, “Cooperative traffic control of a mixed network with two urban regions and a freeway,” Transportation Research Part B: Methodological, vol. 54, pp. 17–36, 2013.

[56] A. Srivastava and W. Jin, “A lane changing cell transmission model for modeling capacity drop at lane drop bottlenecks,” Tech. Rep., 2016.

[57] C. F. Daganzo, “The cell transmission model: A dynamic representation of highway traffic consistent with the hydrodynamic theory,” Transportation Research Part B: Methodological, vol. 28, no. 4, pp. 269–287, 1994.

[58] C. F. Daganzo, “The cell transmission model, part II: network traffic,” Transportation Research Part B: Methodological, vol. 29, no. 2, pp. 79–93, 1995.

[59] M. Kontorinaki, A. Spiliopoulou, C. Roncoli, and M. Papageorgiou, “First-order traffic flow models incorporating capacity drop: Overview and real-data validation,” Transportation Research Part B: Methodological, vol. 106, pp. 52–75, 2017.

[60] M. J. Lighthill and G. B. Whitham, “On kinematic waves II. a theory of traffic flow on long crowded roads,” Proceedings of the Royal Society of London. Series A. Mathematical and Physical Sciences, vol. 229, no. 1178, pp. 317–345, 1955.

[61] P. I. Richards, “Shock waves on the highway,” Operations research, vol. 4, no. 1, pp. 42–51, 1956.

[62] H. Liu, S. Vishnoi, and C. Claudel, “A two-stage stochastic model considering randomness of demand in variable speed limit and boundary flow control,” arXiv preprint arXiv:2110.14025, 2021.

[63] F. L. Hall and K. Agyemang-Duah, “Freeway capacity drop and the definition of capacity,” Transportation research record, no. 1320, 1991.

[64] Y. Zhang and P. A. Ioannou, “Coordinated variable speed limit, ramp metering and lane change control of highway traffic,” IFAC-PapersOnLine, vol. 50, no. 1, pp. 5307–5312, 2017.

[65] X. Li, G. Li, S.-S. Pang, X. Yang, and J. Tian, “Signal timing of intersections using integrated optimization of traffic quality, emissions and fuel consumption: a note,” Transportation Research Part D: Transport and Environment, vol. 9, no. 5, pp. 401–407, 2004.

[66] A. Hajbabaie and R. F. Benekohal, “Traffic signal timing optimization: Choosing the objective function,” Transportation research record, vol. 2355, no. 1, pp. 10–19, 2013.

[67] A. J. Calle-Laguna, J. Du, and H. A. Rakha, “Computing optimum traffic signal cycle length considering vehicle delay and fuel consumption,” Transportation Research Interdisciplinary Perspectives, vol. 3, p. 100021, 2019.

[68] J. A. Bonneson and M. D. Fontaine, “Evaluating intersection improvements: an engineering study guide,” 2001.

[69] U. Epa, “Motor vehicle emission simulator (moves) user guide,” US Environmental Protection Agency, 2010.

# Data Summary

## Products of Research

Vehicle records were collected from each microscopic simulation, and then evaluated the average travel time, the average number of stops and the average emission rates of $CO_2$ using the vehicle records.

## Data Format and Content

All data was compressed into a zip file “CORFLO_project_data.zip”. The “signal_files” folder contains all VISSIM signal files used for the simulation. The “vehicle_records” folder contains vehicle records for all scenarios as well as the linear regression data for the cycle length model. Each vehicle record is a fzp file generated by VISSIM that contains all vehicle information in the specific simulation run. The evaluation results of each case are stored in a csv file in the corresponding subfolder. “scenario0” refers to the no incident scenario. “scenario1” refers to the ramp closure scenario. “scenario2” refers to the lane closure scenario.

In addition, we included the VISSIM model and Python3 scripts for running VISSIM simulations and evaluations in the root folder.

## Data Access and Sharing

All of the above-mentioned data and files are available via Harvard Dataverse under the name “Replication Data for: Coordinated Traffic Flow Control in a Connected Environment”. They can be accessed with the following DOI: https://doi.org/10.7910/DVN/4GK5MW

Suggested citation:

> Yuan, Tianchen, 2023, "Replication Data for: Coordinated Traffic Flow Control in a Connected Environment", https://doi.org/10.7910/DVN/4GK5MW, Harvard Dataverse, V1, UNF:6:+lvklrSrxD5UmsOs18wXjQ== [fileUNF]